Transonic Drag Effect on Vibration Characteristics of Single-Stage Space Vehicles

Ashok Joshi*
Indian Institute of Technology, Bombay 400067, India

Introduction

HIGH-PERFORMANCE space vehicles experience large drag while passing through the atmosphere, and this drag becomes even larger during the transonic regime leading to larger thrust requirements. Vibration analysis procedures for space vehicles usually take into account the effect of propellant mass depletion and predict structural vibration frequencies that are used for designing the flight controls and other systems. However, the presence of a large drag near the nose of the vehicle and an even larger thrust at the tail leads to the development of significant compressive forces that can have a significant effect on the transverse vibration characteristics. Therefore there is a need to take into account the effect of these compressive forces on structural vibration analysis of space vehicles. It is known that compressive forces reduce the effective transverse stiffness and thereby reduce the natural frequency.[1] Therefore, it can be seen that in the presence of compressive forces, along with mass depletion, the transverse frequencies will be significantly lower than the values predicted by considering only the mass depletion effect. The present study investigates the combined effects of compressive forces and the mass depletion on the transverse vibration frequencies of single-stage space vehicles (used henceforth to denote both missiles and rockets). It is assumed that only the wave drag is significant and is concentrated near the nose portion. The space vehicle is structurally modeled as a nonuniform slender beam with both stiffness and mass properties varying along its length. However, the mass depletion is assumed to be uniform along the length of the vehicle, which is nearly the case for single-stage operations. Further, the trajectory with constant thrust is taken and the axial compressive force P is obtained as a sum of the constant drag force term and a variable inertia force term that is derived from the instantaneous acceleration of the vehicle.

Formulation and Solution

Figures 1a and 1b show the configuration of a typical variable geometry space vehicle. The equations of transverse vibration for a slender beam can be based on the elementary beam theory. In the present case, the governing equation has variable coefficients, and only an approximate solution is possible. Therefore, beam functions in finite constant property segments are used for faster convergence of the solution. This simplification leads to a number of governing equations with constant coefficients that can be solved exactly in terms of the beam functions. The nondimensional equation of motion for ith constant beam segment can then be written as

$$\left(\frac{\partial^4 w_i}{\partial \bar{x}_i^4}\right) - a_i\left(\frac{\partial^2 w_i}{\partial \bar{x}_i^2}\right) + \lambda_i^4 w_i = 0 \qquad (1)$$

Here a_i $\{=P(x_i)L_0^2/(EI)_i\}$ is the dimensionless axial compressive force and λ_i $\{=(\rho A)_i\omega^2 L_0^4/(EI)_i\}^{(1/4)}$ is the dimensionless frequency parameter for the ith segment. Here $\bar{x}_i$ takes values from 0 to $\bar{l}_i$ $(=l_i/L_0)$ for all segments where l_i is length of each segment. A new frequency parameter variable λ is defined as

$$\lambda^4 = \left[(\rho A)_0\omega^2 L_0^4/(EI)_0\right] \qquad (2)$$

where ρA_0 $(=M_0/L_0)$ is the average mass per length and EI_0 is the maximum bending rigidity. The compressive force $P(x_i)$ for the ith segment is calculated at its c.g. by summing up the drag D inertia force of all of the segments preceding the current one and taking the average inertia force for the current segment, described by the following expression:

$$P(x_i) = (T/M_0)\sum_{1}^{i-1}(\rho A)_j l_j + 0.5(\rho A)_i l_i + D \qquad (3)$$

The general solution of Eq. (1) can be written as

$$w_i = A_i\cosh\lambda_1\bar{x}_i + B_i\sinh\lambda_1\bar{x}_i + C_i\cos\lambda_2\bar{x}_i + D_i\sin\lambda_2\bar{x}_i \qquad (4)$$

where A_i, B_i, C_i, and D_i are arbitrary constants and λ_1 and λ_2 (roots of the characteristic equation for each segment) are obtained as

$$\lambda_1^2 = \left[\left(a_i^2 + 4\lambda_i^4\right)^{\frac{1}{2}} - a_i\right]/2 \qquad (5)$$

$$\lambda_2^2 = \left[\left(a_i^2 + 4\lambda_i^4\right)^{\frac{1}{2}} + a_i\right]/2 \qquad (6)$$

The transcendental characteristic equation is obtained by applying the boundary and continuity conditions and is represented by a $4N \times 4N$ determinant (N is the number of segments) whose zeros give various values of the frequency parameter λ. Table 1 presents a convergence study to determine the number of segments required to correctly represent the variable coefficient governing equation. For this purpose, the vehicle is successively approximated with a larger number of spanwise segments, and it is seen that convergence is achieved with eight segments.

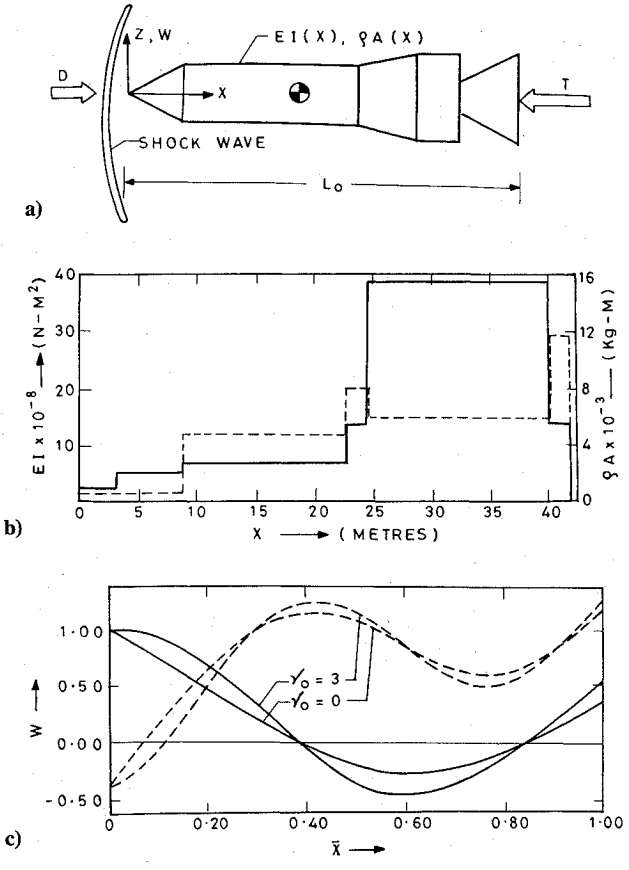

Fig. 1 a) Configuration and geometry of a single-stage space vehicle subjected to thrust and drag; b) ——, the bending rigidity $EI(x)$ and – – –, the mass distribution of a typical single-stage space vehicle; c) ——, first mode and – – –, second mode vibration mode shapes of the typical space vehicle having thrust factor $\beta_0 = 6$, for two values of drag factor $\gamma_0 = 0$ and 6.

Received Dec. 1, 1994; revision received May 10, 1995; accepted for publication May 15, 1995.

*Associate Professor, Department of Aerospace Engineering, Powai.

Table 1 Convergence of the frequency and mode shape solution

Segments	Frequency parameter		Normalized modal mass	
	Mode 1	Mode 2	Mode 1	Mode 2
1	4.1361	7.4199	0.3150	0.2749
2	3.4704	7.0484	0.3892	0.3050
4	5.0017	8.3321	0.3431	0.2209
6	4.9705	8.3954	0.1506	0.1050
8	4.9667	8.3883	0.1510	0.1053

Table 2 Variation of natural frequency of a constant thrust vehicle

a) Having drag and constant mass

β_0	γ_0	Frequency parameter λ	
		Mode 1	Mode 2
0	0	5.2446	8.6038
6	0	5.1168	8.4985
6	1	5.0996	8.4777
6	3	5.0677	8.4353
12	0	4.9667	8.3883
12	2	4.9314	8.3424
12	6	4.8620	8.2450

b) Having drag and variable mass

	Frequency, Hz ($\beta_0 = 12$)			
	$\gamma_0 = 0$		$\gamma_0 = 6$	
$\bar{M}_d$	Mode 1	Mode 2	Mode 1	Mode 2
0.0	2.0049	5.7187	1.9213	5.5250
0.1	2.1133	6.0280	2.0252	5.8238
0.2	2.2415	6.3936	2.1480	6.1771
0.3	2.3963	6.8351	2.2963	6.6036
0.4	2.5883	7.3827	2.4803	7.1327
0.5	2.8353	8.0874	2.7171	7.8135
0.6	3.1700	9.0420	3.0378	8.7358
0.7	3.6604	10.441	3.5077	10.087

Discussion of Results and Conclusions

Table 2a presents the results of the natural frequency of a typical space vehicle (Fig. 1b) subjected to thrust T and drag force variations, in the absence of mass depletion, and it is seen that as thrust factor β_0 $(=T/M_t g)$ is increased from 0 to 12, the value of the frequency parameter λ for the first mode reduces from 5.2446 to 4.9667, a reduction of about 5%. This reduction for second mode is about 4.2%, which is expected. Table 2a also shows that for a given β_0, as the drag factor γ_0 $(=D/M_t g)$ is increased from 0 to 6, the first mode λ reduces further by about 2%. This is the result of an increase in the constant part of the axial compressive force distribution, leading to a lower transverse stiffness. However, this effect is small because of a proportionate reduction in the compressive forces due to inertia. Table 2b shows that the effect of axial compression is decoupled from the effect of mass depletion, resulting in constant percentage reduction in cyclic frequency f, as $\bar{M}_d$ is increased from 0 to 0.7. This is because uniform mass depletion has no impact on the vibration mode shape.

Figure 1c shows a noticeable effect of drag on the vibration mode shapes (obtained for $\beta_0 = 6$ and for two values of γ_0) because the increase in drag changes the axial force distribution affecting the mode shape. Figure 1c shows that the locations of the nodal points for both the mode shapes remain unchanged with the change in the drag. This fact is useful in deciding the sensor locations for control application.

Thus, it can be concluded from the study that, although the effect of transonic drag on the frequency is noticeable, the effect on the vibration mode shapes is substantial, and this can have significant effect on the aeroelastic characteristics and control implementation. Therefore, it is considered important that effects of both the axial compression and transonic drag are taken into account while predicting the free vibration characteristics of single-stage space vehicles.

Reference

[1]Joshi, A., and Suryanarayan, S., "Unified Analytical Solution for Various Boundary Conditions for the Coupled Flexural-Torsional Vibration of Beams Subjected to Axial Loads and End Moments," *Journal of Sound and Vibration*, Vol. 129, No. 2, 1989, pp. 313–326.

R. M. Cummings
Associate Editor

Russian RD-704 for Single-Stage Vehicles

James A. Martin,* Thongsay Vongpaseuth,† and G. Venkatasubramanyam‡
University of Alabama, Tuscaloosa, Alabama 35487-0280

Introduction

THE Space Shuttle has been a useful vehicle for a number of missions. It has not, however, lived up to hoped for reductions in the cost of space transportation. Current efforts in the government and aerospace industry are focusing on advanced concepts that could provide reduced launch costs and improved operations. One concept being considered is the single-stage-to-orbit (SSTO) vehicle that might allow less complex operations than concepts involving staging or expendable hardware.

The SSTO is technically challenging because the ideal velocity required to achieve orbit is nearly the maximum possible from a single stage. Any improvement in the SSTO is therefore magnified. One propulsion scheme that has been shown to provide an advantage[1–6] is the use of two fuels, one with high density and one with high specific impulse, together with oxygen. Such a tripropellant vehicle benefits from the smaller tanks and lighter engines allowed by the high-density fuel while retaining the advantage of high specific impulse for the final portion of the ascent trajectory.

One approach to a tripropellant vehicle is to use a single engine type that operates with two fuels, or a tripropellant engine. To gain the advantage of the high-density fuel early in the flight without losing the advantage of high specific impulse later in the flight, it is important that the engine operate in two modes: the first mode must get most of the thrust from the high-density fuel, whereas the second mode must use essentially only the high specific impulse fuel.

The Russian RD-170 engine has been used successfully as a kerosene and oxygen engine, and it has good performance for a high density fuel such as kerosene. The RD-704 (Fig. 1) is a design that is based on the proven RD-170 with the addition of hydrogen fuel and a second operating mode. There are several design parameters for the RD-704 that have not been fully studied and that might have had a significant effect on the performance of the RD-704 on an SSTO. The purpose of this study was to examine some of these parameters and find near-optimum values. Most important was the question of whether a two-position nozzle could provide an improvement that would justify the complexity and development cost needed. This part of the study required consideration of the best expansion ratios for both the fixed nozzle and the nozzle extension. Additional parameters in the study were the best hydrogen flow during mode 1 and the best mixture ratio during mode 2.

Received June 1, 1995; presented as Paper 95-2952 at the AIAA/ASME/SAE/ASEE 31st Joint Propulsion Conference and Exhibit, San Diego, CA, July 10–12, 1995; revision received Oct. 27, 1995; accepted for publication Nov. 3, 1995.

*Associate Professor, Department of Aerospace Engineering. Associate Fellow AIAA.

†Graduate Student, Department of Engineering Science and Mechanics. Student Member AIAA.

‡Graduate Student, Department of Aerospace Engineering. Student Member AIAA.